Shock Temperatures and Melting of Iron at Earth Core Conditions

C. S. Yoo, N. C. Holmes, and M. Ross
Lawrence Livermore National Laboratory, Livermore, California 94551
D. J. Webb and C. Pike
Physics Department, University of California, Davis, California 95616
(Received 13 October 1992)

The temperature of shock compressed iron has been measured to 340 GPa, using well characterized iron films sputtered on transparent diamond substrates and a 1 ns time-resolved optical method. We find a knee on the (P,T) iron Hugoniot indicating melting at 6350 K and 235 GPa and at 6720 K and 300 GPa. An extrapolation yields an iron melting temperature of 6830 ($\pm$ 500) K at 330 GPa, the pressure of the Earth inner-outer core boundary. Implication of the melting data for the iron phase diagram is also discussed.

PACS numbers: 62.50.+p, 64.70.Dv

The phase diagram of iron, in addition to being of intrinsic scientific interest, provides a critical constraint for modeling the chemical composition and energy balance of the Earth's core. The Earth's core contains mostly iron distributed in two layers: the solid inner layer of nearly pure iron and the liquid outer layer of iron alloys with lighter elements like S, O, H, Si, Mg, etc. Thus, the iron melting temperature at the pressure of the Earth inner-core and outer-core boundary (IOB), 330 GPa, may provide an upper bound for the temperature. The recrystallization of iron occurring at the boundary releases latent heat and gravitational energy which provide the heat necessary for convection in the outer core and produce Earth's magnetic field [1].

Current Earth core models rely strongly on extrapolations of the melting data of iron from below 100 GPa. However, these extrapolations not only give a large uncertainty in the IOB temperature ranging from 4000 to 9000 K [1], but also yield phase diagrams that are qualitatively different from one another at the IOB conditions [2,3]. For example, the melting temperature reported by Williams and co-workers [2] increases rapidly with pressure, the extrapolation of which results in a ε-γ-liquid iron triple point at the IOB pressure 330 GPa and 7600 K. On the other hand, Boehler, von Bargen, and Chopelas [3] present the ε-γ-liquid triple point at the substantially lower pressure of 100 GPa and 2800 K and suggest an IOB temperature near 4200 K. Recently, the situation has become confused even further by the findings of Boehler [4] and Saxena, Shen, and Lazor [5] of a new solid phase of unknown structure in what has been believed to be the stability field of the ε phase. Brown and McQueen [6] have observed two discontinuous changes of the iron sound velocity at shock pressures of 200 and 240 GPa, which are attributed to phase transitions of iron and the latter to melting. However, the temperatures were not measured, but were estimated from the shock energy to be 5800 $\pm$ 500 K at the IOB pressure.

A direct method for obtaining melting temperatures above a megabar and several thousand degrees is by measuring shock temperatures [7]. This is typically done by optical pyrometry, which measures the thermal radiation of shocked materials at several discrete wavelengths. However, difficulties are introduced in the case of nontransparent materials like metals, because of a thin optical penetration depth $\sim$20 nm and a short shock wave transit time over this distance $<$ 1 ps. For this reason and because of the rarefaction wave which rapidly releases the iron pressure to ambient conditions at the free surface, an optical window is typically placed against the surface of the metal film to retain the shock state for a longer time period. In this case, thermal radiation is measured from the metal/window interface, which then introduces several issues that must be addressed to obtain a reliable shock temperature. Those include characterization of the iron film and iron film/window interface, optical property changes of window materials at high pressures and temperatures, and thermal conduction occurring across the interface [8].

The optical method measuring shock temperatures has previously been applied for iron by Ahrens and coworkers [2,9]; however, the measured shock temperatures have considerable scatter [9] and show no clear indication of melting. In their analysis, because of possible sample defects such as sample porosity and an imperfect sample/window interface that would result in anomalously high shock temperatures with large scatter, they have used only a small portion of the data yielding the lowest temperature at any given pressure. Later, incorporating these data with the data of Williams *et al.* [2], the iron melting temperature was reported to be 7600 $\pm$ 500 K at 330 GPa. The data scatter in the shock temperature is in part due to unknown characteristics of iron samples, optical window materials, and the iron-window interface. In this work we address these issues experimentally and present new shock temperature data showing a clear indication of melting.

Iron films ($\sim$2 μm thick) were prepared by sputtering onto diamond substrates held at 300 °C. The elevated substrate temperature was chosen to give good film adhesion while minimizing the thickness of the iron/diamond interface. The iron initially wet the diamond sur-

0031-9007/93/70(25)/3931(4)$06.00

face well, so that no gaps or voids are present in a 100 Å thick film. The density of iron films differs from that of a bulk crystal by less than 1%, which is within our instrumental resolution [10]. Auger depth profiling analysis, monitoring both carbon and iron simultaneously, was used to estimate the interface zone to be about 50 Å in thickness. This is substantially thinner than the optical penetration depth of iron ~200 Å and assures that the thermal radiation measured at the interface is characteristic of iron shock temperatures.

The iron film/diamond sample is sandwiched between a diamond-turned iron baseplate and a sapphire disk. This configuration stems from the requirements to obtain a well determined iron shock state, to minimize any thermal disturbance generated from a direct impact on an iron film, and to provide mechanical strength for the sample. The final iron target assembly is then kept in high vacuum prior to the gas gun experiment to preclude rust or oxidation of the iron surface.

The shock wave is generated by impacting a Ta disk on the iron baseplate using a two-stage gas gun [11]. Shock pressures are determined using the impedance matching method and the equations of state for Ta [12] and iron [6] that are accurately known. Thermal emission from the iron/diamond interface is measured using a fast time-resolved emission system similar to one described previously [13]. A multichannel optical fiber delivers the emission to two detection systems: (1) a streak camera system records a quasicontinuous spectrum between 350 and 700 nm every 1.8 ns for a 100 ns time period, which is long enough to cover the shock events of interest, and (2) a photomultiplier tube (PMT) system records time-resolved emission intensity at six discrete wavelengths. Because the optical fiber collects the emission from only a small central area of the sample (<1 mm), the shock state of the sampling area is well defined in one dimension and, thus, provides a fast time resolution that primarily depends on the rise time of the recording electronics. Time and spectral resolution of the system are approximately 1 ns and 2 mm, respectively.

Typical time-resolved emission spectra of the shocked iron are shown in Fig. 1. The intensity rise at 455 ns (a) is due to the shock-wave arrival at the iron/diamond interface. The broad nature of the spectra suggests that the emission is thermal. The emission intensity remains nearly constant within a few percent during the shock wave transits through the diamond window, indicating that the optical properties of the shocked diamond remain unchanged. This and other experiments reported here suggest that diamond is transparent in the entire pressure range to 300 GPa. The experiment is completed when the shock wave enters the sapphire disk at 483 ns (b), where the emission intensity rapidly decreases. This is likely due to partial opacity of the shocked sapphire [13]. We have also observed a transient increase of the emission intensity at 489 ns in the sapphire, whose nature has not been clearly characterized as yet.

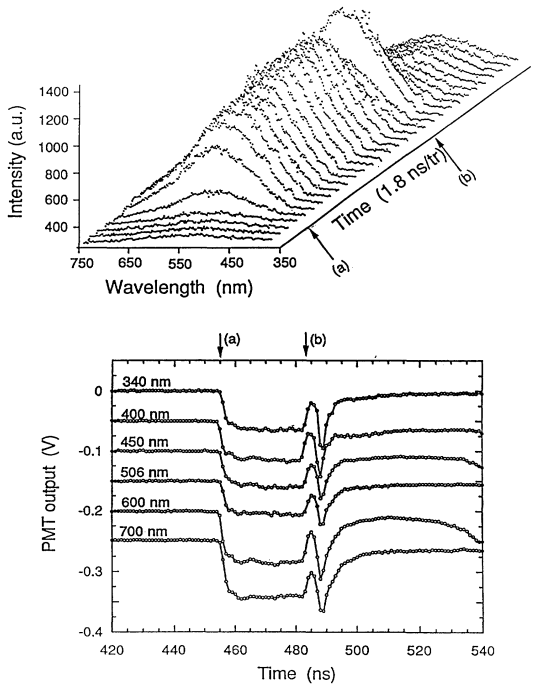

FIG. 1. Time-resolved thermal emission spectra recorded by the streaking camera system (top) and PMT system (bottom). The emission is measured from the iron/diamond interface, and the pressures of the iron and diamond (or in the interface) are 313 and 255 GPa, respectively.

The interface temperature T_i is determined by fitting the measured emission intensity to a grey-body radiation equation. However, due to thermal conduction occurring from shocked hot iron to shocked, but relatively cold, diamond, T_i is considerably lower than the shock temperature of iron. A one-dimensional thermal conduction model [14] is used to obtain the temperature profiles in diamond and iron and at the interface:

$$\frac{\delta}{\delta x}\left(\kappa\frac{\delta T}{\delta x}\right)=\frac{1}{\rho C}\frac{\delta T}{\delta t}, \tag{1}$$

where κ, ρ, and C, respectively, represent the thermal conductivity, density, and heat capacity. In the case where the thermal conductivity κ is independent of temperature, one can obtain a simple solution converting the T_i to the release shock temperature of iron, T_r [15,16]:

$$T_i=T_r+(T_d-T_r)/(1+\alpha), \tag{2}$$

$$\alpha=[\kappa_r\rho_r C_r/\kappa_d\rho_d C_d]^{1/2}. \tag{3}$$

Here, the subscripts d and r denote the shocked diamond and the released iron.

The thermal conductivity of iron is approximated by the Wiedeman-Franz law using a linear scaling of the electrical conductivity measured along the Hugoniot [17, 18]. The high temperature thermal conductivity values for diamond have previously been measured to 1200 K [19,20], and the results have been precisely described by

a phonon scattering model [21]. A similar model is used to obtain the thermal conductivity of diamond at high temperature and pressures. Here, the pressure-dependent Debye temperature and phonon frequency of diamond are obtained from the Debye-Grüneisen approximation [22,23]. The densities of iron and diamond are obtained from previously reported P-V Hugoniots [6,24,25]. The heat capacity of iron is obtained by Dulong-Petit approximation $3R$, and that of diamond is calculated by an Einstein model [26].

The major uncertainty of the thermal analysis described above arises from the diamond thermal conductivity which strongly depends on pressure and particularly temperature. For example, a several μm thick layer of diamond in contact with the shock-heated iron is at substantially higher temperature than the shock temperature of bulk diamond. The conductivities of diamond at ambient pressure decrease from about 300 W/m K at 1000 K to about 30 W/m K at 1000 K. Therefore, it is necessary to solve Eq. (1) using temperature-dependent thermal conductivity. Diamond and iron specimens were divided into many layers of 1 μm thick slabs that are in perfect thermal contacts, and Eq. (1) was solved numerically in each microslab and boundaries at a given pressure. The temperature profiles of diamond and iron are calculated at 1 ns time steps, and the thermal conductivities are evaluated according to these profiles. The final shock temperature greatly depends on these thermal corrections, which can vary the final temperature by (10–20)%.

The shock temperature T_h of iron on the principal Hugoniot is determined from the released shock temperature T_r by a Mie-Grüneisen thermal relation:

$$T_h = T_r \exp\left(\int_{V_h}^{V_r} \frac{\gamma}{V} dV\right), \quad (4)$$

where the γ and V are the Grüneisen parameter and specific volume of iron, respectively. We approximate $\gamma/V = 16.6$ [6]. Because of a good shock impedance match between diamond and iron at the pressure range of interest, this correction is typically less than 5%.

Figure 2 presents the measured shock temperatures of iron between 150 and 340 GPa, together with the previous measurements [2,9]. The measured temperatures systematically increase with increasing pressure and clearly show an inflection at the pressure region between 235 and 300 GPa, which we attribute to melting and which is consistent with the shock anomaly pressure of 243 GPa previously observed in the sound velocity measurements and also interpreted as melting. The present measurements are in agreement with those reported previously below 250 GPa, but are substantially lower at higher pressures. The previous works also failed to observe any break in the Hugoniot temperature at melting. Based on our measurements we estimate the melting temperature at the Earth IOB pressure 330 GPa to be 6830 K, lower than the previous estimate of 7600 K. On the other hand, the present melting data are still higher than

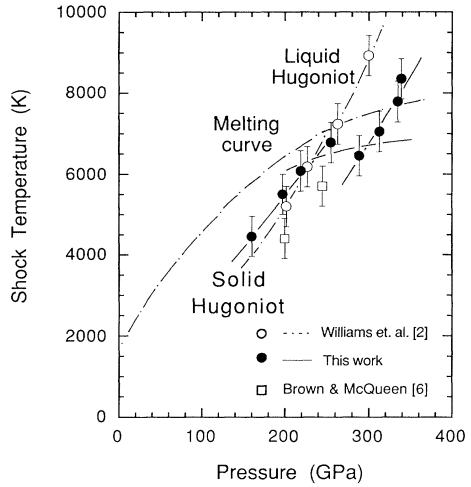

FIG. 2. Iron shock temperatures (solid circles and solid lines) between 150 and 340 GPa, in comparison with the previous measurements (open circles and dash-dotted lines) by Williams *et al.* [2]. The open squares indicate the shock anomaly points [6].

the earlier estimates of Brown and McQueen's 5000–5700 K at 243 GPa and of 5800 K at 330 GPa [6].

It is of some interest to understand how the present work fits in with static studies of the iron phase diagram below 100 GPa, based on laser heating experiments [2,3,27,28]. The iron phase diagram is relatively well known at low pressures below 20 GPa [29]. However, the melting temperatures above 20 GPa show a significant discrepancy among the different measurements [2–5], which results in at least the two plausible, but mutually exclusive, iron phase diagrams as shown in Fig. 3. Based on the extrapolations of the melting lines of these static data, iron melting temperature at 200 GPa could be in a wide temperature range between 6000 and 3800 K, illustrating the large disagreement of static melting temperatures.

The iron melting temperatures as determined by shock temperatures are substantially higher than the extrapolation of Boehler's melting line, but appear to be consistent with that of Williams *et al.* The data of Williams *et al.* interpret the 200 and 243 GPa anomalies as the ε- to γ-iron transition and the γ- to liquid iron, respectively; whereas, in Boehler's data the transition at 200 GPa could be explained in terms of a transition from the ε phase to a new α' (bcc) phase which has been proposed theoretically by Ross, Young, and Grover [30], except that Boehler's temperatures are significantly lower. However, Saxena, Shen, and Lazor [5] have suggested that the α' phase appears at low temperatures, which means there must be an additional phase at high temperatures to explain the 200 GPa shock anomaly point [6]. Recently, a molecular dynamics simulation by Matsui [31] has shown that iron transforms from the ε phase to a bcc phase at 300 GPa and 5000 K with a 0.5% volume decrease.

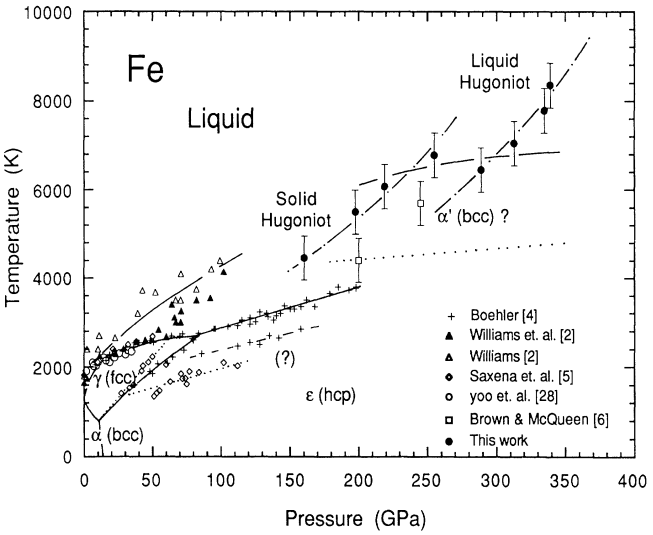

FIG. 3. Iron phase diagram based on this work (solid circles) and previous laser heating works [2–5,28,29]. The theoretically proposed α' (bcc) phase whose phase line coincides with the shock anomaly pressure at 200 GPa (open square [6]) is also reproduced (dotted line) [30]. The recently discovered new phase boundaries in what has been believed to be the ε-phase stability zone are also reproduced by dashed [4] and dotted [5] lines. The δ phase also occurs along the low pressure melting line between 1650 and 1800 K at 0 GPa, but is not shown in the figure for clarity.

The major result of this work is an experimentally determined melting point for iron at 235 GPa and 6350 K and an estimated upper bound for the Earth's IOB temperature 6830 K $\pm$ 500 K at 330 GPa. However, a major discrepancy exists between the shock and static melting data. For example, Boehler's static melting temperatures are sufficiently lower than those determined by shock temperatures, which would mean that the Hugoniot points reported here and two shock anomalies reported previously [6] are in the liquid phase, which is unlikely.

We thank Erv See, Jim Crawford, and Sam Weaver for the experimental assistance, and Bill Nellis and David Young for valuable discussions. This work has been performed under the auspices of the U.S. Department of Energy by Lawrence Livermore National Laboratory under Contract No. W-7405-ENG-48.

[1] O. L. Anderson, J. Geophys. Res. **95**, 21 697 (1990).
[2] Q. Williams, R. Jeanloz, J. Bass, B. Svendsen, and T. J. Ahrens, Science **236**, 181 (1987).
[3] R. Boehler, N. von Bargen, and A. Chopelas, J. Geophys. Res. **95**, 21 731 (1990).
[4] R. Boehler (to be published).
[5] S. K. Saxena, G. Shen, and P. Lazor (to be published).
[6] J. M. Brown and R. G. McQueen, Geophys. Res. Lett. **7**, 533 (1980); J. Geophys. Res. **91**, 7485 (1986).
[7] S. B. Kormer, Usp. Fiz. Nauk. **94**, 641 (1968) [Sov. Phys. Usp. **11**, 229 (1968)].
[8] W. J. Nellis and C. S. Yoo, J. Geophys. Res. **954**, 21 749 (1990).
[9] J. D. Bass, B. Svendsen, and T. J. Ahrens, in *High Pressure Research in Mineral Physics,* edited by M. H. Manghnani and Y. Syono (American Geophysical Union, Washington, DC, 1987), pp. 393–402 and 402–423.
[10] For each film we measured the volume to better than 1% and weighted the film to better than 1%. We also checked the weight by measuring the magnetization to about 2% accuracy.
[11] A. H. Jones, W. M. Isbell, and C. J. Maiden, J. Appl. Phys. **37**, 3493 (1966).
[12] N. C. Holmes, J. A. Moriarty, G. R. Fathers, and W. J. Nellis, J. Appl. Phys. **66**, 2962 (1989).
[13] C. S. Yoo, N. C. Holmes, and E. See, in *Shock Waves in Condensed Matter—1991,* edited by S. C. Schmidt, R. D. Dick, J. W. Forbes, and D. G. Tasker (North-Holland, Amsterdam, 1992), p. 733.
[14] H. S. Carslaw and J. C. Jaeger, in *Conduction of Heat in Solids* (Clarendon, Oxford, 1959), Chap. XI, pp. 239–271.
[15] R. Gover and P. A. Urtiew, J. Appl. Phys. **45**, 146 (1974).
[16] R. G. McQueen and D. G. Isaak, J. Geophys. Res. **95**, 21 753 (1990).
[17] R. N. Keeler, in *Physic of High Energy Density,* Proceedings of the International School of Physics "Enrico Fermi," Course XLVIII, edited by P. Caldrirola and H. Knoepfel (Academic, New York, 1971), p. 106.
[18] G. Matassov, Ph.D. thesis, University of California [Lawrence Livermore National Laboratory Report No. UCRL-52322 (unpublished)].
[19] R. Berman, P. R. W. Hudsen, and M. Martinez, J. Phys. (Paris), Lett. **8**, L430 (1975).
[20] J. W. Vandersande, C. B. Vining, and A. Zoltan, in *Proceedings of the Second International Symposium on Diamond Materials,* edited by A. J. Purdes, B. M. Meyerson, J. C. Angus, K. E. Spear, R. F. Davis, and M. Yoder (Electrochemical Society, Inc., Pennington, NJ, 1991), p. 443.
[21] D. G. Onn, A. Witek, Y. Z. Qiu, T. R. Anthony, and W. F. Banholzer, Phys. Rev. Lett. **68**, 2806 (1992).
[22] M. C. Roufosse and R. Jeanloz, J. Geophys. Res. **88**, 7399 (1983).
[23] T. J. Shankland, J. Geophys. Res. **77**, 3750 (1972).
[24] K. Kondo and T. J. Ahrens, Geophys. Res. Lett. **10**, 281 (1983).
[25] M. Pavloskii, Fiz. Tverd. Tela (Leningrad) **13**, 893 (1971) [Sov. Phys. Solid State **13**, 741 (1971)].
[26] M. van Thiel and F. H. Ree, Int. J. Thermophys. **10**, 227 (1989).
[27] C. S. Yoo, J. Akellar, and C. Ruddle, EOS Trans. Am. Geophys. Union 64 (1992).
[28] P. Lazor, G. Shen, and S. K. Saxena, Phys. Chem. Mineral. (to be published).
[29] L. G. Liu and W. A. Bassett, in *Elements, Oxidex and Silicate: High Pressure Phases with Implications for the Earth's Interior* (Oxford Univ. Press, New York, 1986), p. 52.
[30] M. Ross, D. A. Young, and R. Grover, J. Geophys. Res. **95**, 21 713 (1990).
[31] M. Matsui, Central Core Earth **2**, 79 (1992).